Australian Meteorological and Oceanographic Journal 61 (2011) 125-135

Seasonal climate summary southern hemisphere (winter 2010): a fast developing La Niña

Catherine Ganter
National Climate Centre, Bureau of Meteorology, Australia

(Manuscript received May 2011)

Southern hemisphere circulation patterns and associated anomalies for the austral winter 2010 are reviewed, with emphasis given to the Pacific Basin climate indicators and Australian rainfall and temperature patterns. Winter 2010 saw the fast development of La Niña conditions across the Pacific Basin, a rapid transition from the El Niño conditions in place during summer 2009–10. By the end of winter 2010, most ENSO indices were displaying a La Niña signal, with the equatorial Pacific Ocean surface and sub-surface cooling during each month of winter. The Southern Oscillation Index (SOI) became more positive over winter, with an August value of +18.8. In the extra-tropics, a very strong positive phase of the Southern Annular Mode (SAM) was in place for most of winter 2010, with June and July both recording their highest positive monthly SAM index values on record. In the Australian region, rainfall was generally average to above average. However, in contrast to the rest of the continent, southwest Western Australia had its driest winter in 111 years of records. Temperatures tended to be cooler than normal across southern Australia, and warmer than normal in northern Australia.

Introduction

This summary reviews the southern hemisphere climate patterns for the austral 2010 winter (June to August). Australasian and Pacific regions are given particular attention in this discussion. The main sources of information for this summary were analyses prepared by the Australian Bureau of Meteorology's National Climate Centre and the Centre for Australian Weather and Climate Research (CAWCR).

ENSO and Pacific Basin climate indices

The Troup Southern Oscillation Index (SOI)[1]

The Troup Southern Oscillation Index (SOI) for the period January 2006 to August 2010 is shown in Fig. 1, together with a five-month weighted moving average. The SOI is calculated using the mean sea-level pressure (MSLP) from both Darwin and Tahiti. Persistent departures of the SOI from zero can reflect El Niño-Southern Oscillation (ENSO) events.

At the beginning of 2010, El Niño conditions were in place (Tobin 2010). Autumn brought a rapid rise in the SOI, ending the El Niño and beginning the transition to a La Niña. Winter values of the SOI were all positive, with a +1.8 for

Fig. 1 Southern Oscillation Index, from January 2006 to August 2010, together with a five-month binomially weighted moving average. Means and standard deviations used in the computation of the SOI are based on the period 1933–1992.

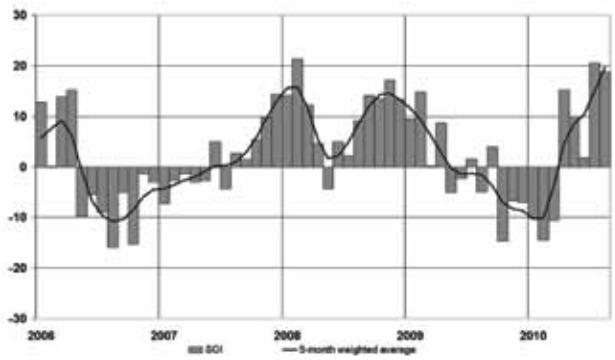

[1]The Troup Southern Oscillation Index (Troup 1965) used in this article is ten times the standardised monthly anomaly of the difference in mean sea-level pressure (MSLP) between Tahiti and Darwin. The calculation is based on a sixty-year climatology (1933-1992). The Darwin MSLP is provided by the Bureau of Meteorology, with the Tahiti MSLP being provided by Météo France inter-regional direction for French Polynesia.

Corresponding author address: Catherine Ganter, National Climate Centre, Bureau of Meteorology, GPO Box 1289, Melbourne Vic. 3001, Australia
Email: c.ganter@bom.gov.au

June, +20.5 for July and +18.8 for August. The winter MSLP values at Darwin were generally slightly below the long-term average. The monthly anomalies (based on the period 1933–1992) for June, July and August in Darwin were +0.7, –0.7 and –0.6 hPa, respectively, while the corresponding Tahiti MSLP values were above average, with +0.9, +2.4 and +2.4 hPa for the winter months. While both sites contributed to the rise in SOI, the above average values at Tahiti had a greater effect.

Composite monthly ENSO index

A composite monthly ENSO index, calculated as the standardised amplitude of the first principal component[2] of monthly Darwin and Tahiti MSLP[3] and monthly NINO3, NINO3.4 and NINO4 sea-surface temperatures[4] (SSTs) (Kuleshov et al. 2008), continued a switch to negative values which began in April 2010 (Fig. 2). Two of the three winter values well exceeded one standard deviation, confirming that the increasing positive phase of the Southern Oscillation had reached La Niña proportions.

Fig. 2 Composite standardised monthly ENSO index from January 2006 to August 2010, together with a weighted three-month moving average. See text for details.

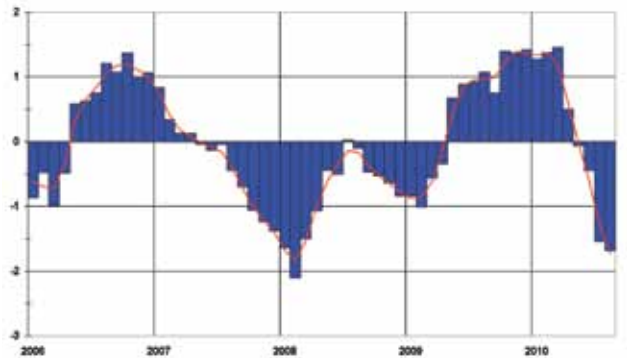

Multivariate ENSO index

The Multivariate ENSO Index[5] (MEI), produced by the US Climate Diagnostics Center, is derived from a number of atmospheric and oceanic parameters typically associated with ENSO and is calculated as a two-month mean (Wolter and Timlin 1993, 1998). Significant negative values indicate La Niña, while significant positive values indicate El Niño. The MEI values have been ranked over the 61 year record, beginning in 1950. The lowest value (1) signifies the strongest La Niña case for that particular two month pairing, while the highest number (61) signifies the strongest El Niño case. At the beginning of the year, the January–February 2010 pair was +1.502, ranked 57 (fifth strongest El Niño value). By May–June this had plummeted to –0.412, and ranked 16 (weak La Niña conditions), and the June–July value was –1.166 (ranked ninth). The value of July-August was ranked 2 (–1.810), indicating that the 2010 La Niña could be one of the strongest in the MEI history (Climate Diagnostics Center 2010).

Outgoing long-wave radiation

Outgoing long-wave radiation (OLR) over the equatorial Pacific near the date-line (5°S to 5°N and 160°E to 160°W) is a good measure of tropical deep convection, with increases (decreases) in OLR indicating decreases (increases) in convection. During La Niña events, OLR is often increased, meaning convection is often suppressed over this region. El Niño events on the other hand, usually have decreased OLR, meaning convection is generally enhanced over this region. The Climate Prediction Center, Washington, computes a standardised monthly anomaly[6] of OLR over the equatorial Pacific. Monthly values for June, July and August were +1.2, +1.2 and +1.3, respectively. The seasonal mean for winter was +1.2, the third highest winter value on record (records began in 1974). The strongly positive values are consistent with La Niña conditions, and indicate that there was decreased convection over the equatorial Pacific.

The spatial pattern of seasonal OLR anomalies across the Asia-Pacific tropics for winter 2010 is shown in Fig. 3. Consistent with the standardised anomalies discussed above, very strong positive anomalies were present in the equatorial Pacific, just west of the date-line. Very strong negative OLR anomalies were present over Indonesia, indicating that there was strongly anomalous convection

Fig. 3 OLR anomalies for winter 2010 in W m^{-2}. Base period is from 1979 to 1998. The mapped region extends from 40°S to 40°N and from 70°E to 180°E.

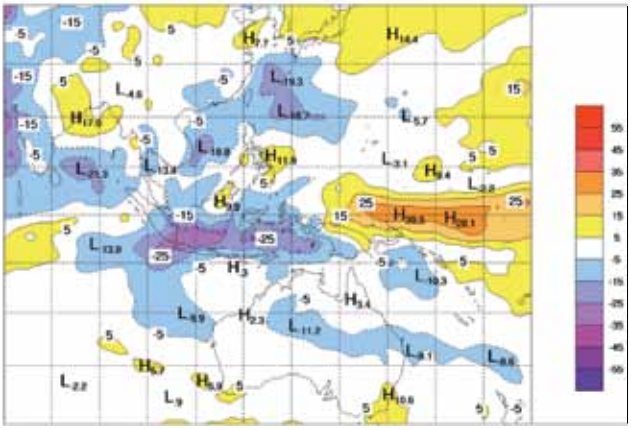

[2]The principal component analysis and standardisation of this ENSO index is performed over the period 1950–1999.
[3]MSLP data obtained from http://www.bom.gov.au/climate/current/soihtm1.shtml. As previously mentioned, the Tahiti MSLP data are provided by Météo France inter-regional direction for French Polynesia.
[4]SST indices obtained from ftp://ftp.cpc.ncep.noaa.gov/wd52dg/data/indices/sstoi.indices.
[5]Multivariate ENSO Index obtained from http://www.esrl.noaa.gov/psd/people/klaus.wolter/MEI/table.html. The MEI is a standardised anomaly index.

[6]Standardised monthly OLR anomaly data obtained from http://www.cpc.ncep.noaa.gov/data/indices/olr

over the region during June to August. This pattern is well aligned with that expected during La Niña events. Negative OLR anomalies were also present over central Australia, which experienced a much wetter than normal winter.

Madden-Julian Oscillation

The Madden-Julian Oscillation (MJO) is a tropical atmospheric anomaly which develops in the Indian Ocean and propagates eastwards into the Pacific Ocean (Donald et al. 2004). The MJO takes approximately 30 to 60 days to reach the western Pacific, with a frequency of six to twelve events per year (Donald et al. 2004). When the MJO is in an active phase, it is associated with increased tropical convection, with the effects at this time of year concentrated in the northern hemisphere. The evolution of tropical convection anomalies along the equator with time is shown in Fig. 4, starting from May 2010 through to November 2010. In the daily averaged OLR anomalies in Fig. 4, June to August 2010 was a weak period for the MJO. However, one brief eastward-propagating band of tropical convection was evident during early July, when an eastward-propagating band of MJO related convection was located in the Indian Ocean. By mid to late July the band had moved into Australian longitudes before weakening and becoming indiscernible. This MJO band did not extend into the western Pacific.

As discussed in the previous section, positive OLR anomalies over the central equatorial Pacific may also be seen in Fig. 4. These positive anomalies are associated with La Niña conditions, and became established during autumn.

Fig. 4 Time-longitude section of 7-day running mean OLR anomalies, averaged for 7.5°S–7.5°N, for the period May 2010 through to November 2010. Anomalies are with respect to a base period of 1979–2001.

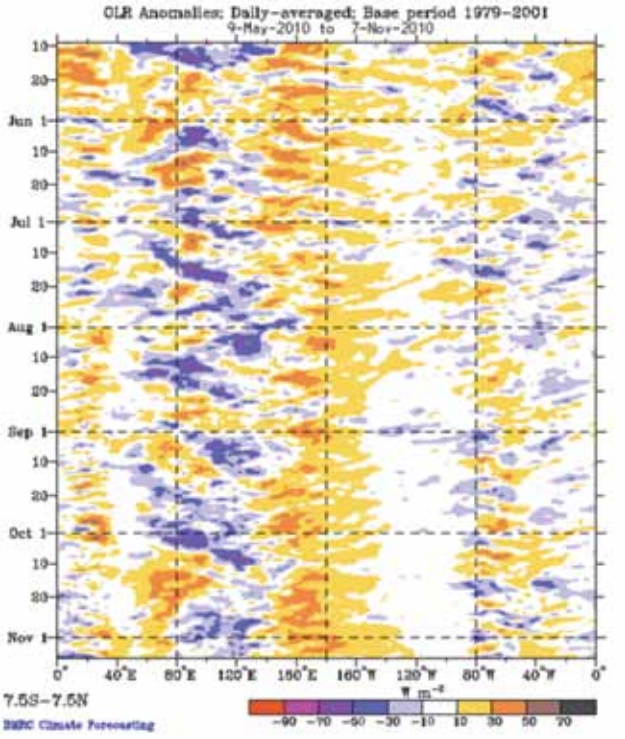

Oceanic patterns

Sea-surface temperatures

Winter 2010 global sea-surface temperature (SST) anomalies, from the US National and Oceanic and Atmospheric Administration Optimum Interpolation analysis (Reynolds et al. 2002), are displayed in Fig. 5, in degrees Celsius (°C). Positive (warm) anomalies are shown in red shades, while negative (cool) anomalies are shown in blue shades. During autumn, the SSTs were in a transition state, with the 2009–10 El Niño breaking down (Campbell 2011). The equatorial Pacific cooled rapidly during each month of winter, with the overall winter pattern being that of an emerging La Niña. Peak SST anomalies of between –1.5 °C to –2.0 °C were predominantly located in the far eastern Pacific, while anomalies of –1.0 °C to –1.5 °C extend into the central Pacific.

All three standard monthly NINO indices were negative by the end of winter. In the eastern Pacific, the NINO3 index cooled significantly from +0.18 °C in May to –0.55 °C in June to –0.99 °C in August. Similarly, in the central Pacific, NINO 3.4 also cooled over winter, from –0.53 °C in June to –1.21 °C

Fig. 5 Global anomalies of sea-surface temperature (SST) for winter 2010 in °C. The contour interval is 0.5 °C, and the base period is 1961–1990.

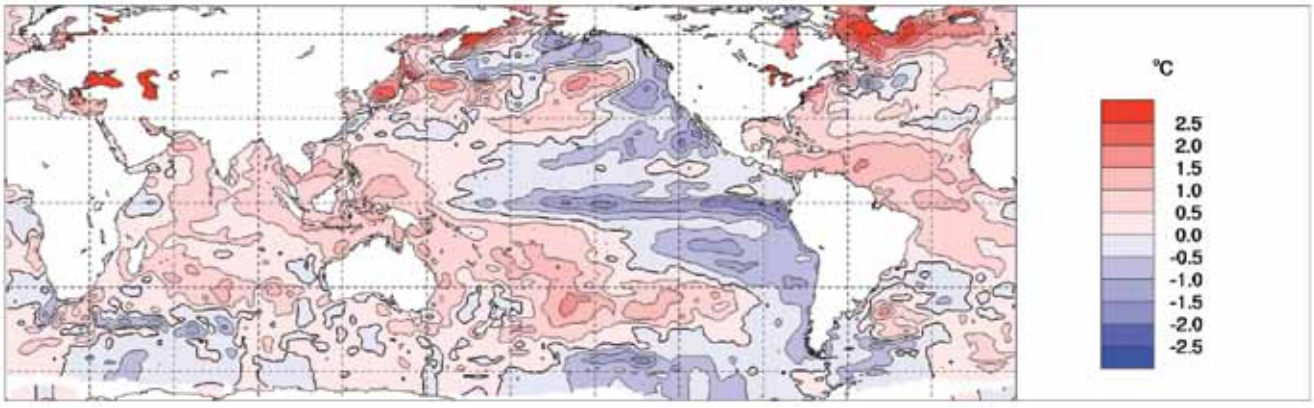

in August. NINO4, located in the central to western Pacific, was neutral in June (+0.06 °C), cooling to an August value of –0.92 °C. The largest cooling occurred between May and June for NINO3 and NINO 3.4, where the two regions cooled by 0.7 °C and 0.6 °C, respectively, while for NINO4 the largest cooling was 0.5 °C, between June and July.

SSTs were also above average across the tropical Indian Ocean, except a small region near the African coast. For most of winter, the Indian Ocean Dipole (IOD) was neutral, except during August when the IOD became negative, falling below the –0.4 °C threshold from mid-August. In the Australian region (a box from 0ºS to 50ºS and 94ºE to 174ºE), SSTs were particularly warm. For winter, the Australian region SSTs were second warmest on record, behind 1998. Of particular note, the Australian region experienced its warmest June SSTs on record, with an anomaly of +0.57 °C.

Subsurface ocean patterns

The Hovmöller diagram for the 20 °C isotherm depth anomaly along the equator from January 2001 to August 2010, obtained from NOAA's TAO/TRITON data[7], is shown in Fig. 6. The 20 °C isotherm depth is generally located close to the equatorial thermocline, which is the region of greatest temperature gradient with depth, and is the boundary between the warm near-surface and cold deep-ocean waters. Therefore, measurements of the 20 °C isotherm depth make a good proxy for the thermocline depth. Positive (negative) anomalies correspond to the 20 °C isotherm being deeper (shallower) than average. Changes in the thermocline depth may act as a precursor to subsequent changes at the ocean surface. A shallow thermocline depth results in more cold water available for up-welling, and therefore a potential cooling of surface temperatures.

Fig. 6 Time-longitude section of the five-day 20 °C isotherm depth anomalies at the equator (2°S–2°N) from January 2001 (top of plot) to August 2010 (bottom). Units are in metres.

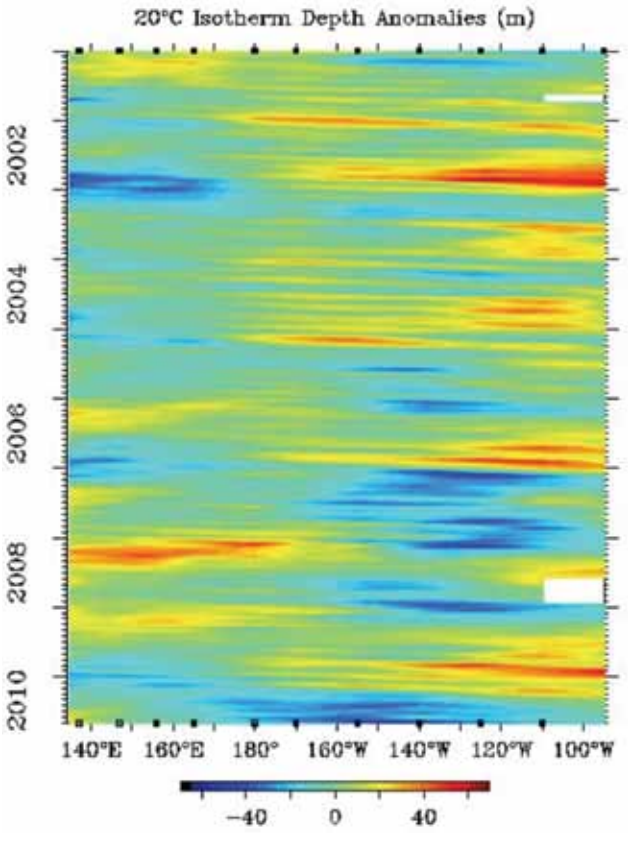

In late 2009 and early 2010 a mature El Niño event was in place: the 20 °C isotherm anomaly was positive in the central and eastern Pacific, while there were weak negative anomalies in the western Pacific. Through autumn the sub-surface cooled across the central and eastern Pacific, while the far western Pacific warmed slightly, although remaining on the cool side of normal. Winter continued this warming/cooling trend, with the central to eastern Pacific developing strongly negative 20 °C isotherm anomalies, while the far western Pacific developed weak positive anomalies. It is possible that the cool anomalies were influenced by the eastward propagation of an up-welling Kelvin wave. The pattern of a shallower-than-normal 20 °C isotherm in the central and eastern Pacific and a deeper-than-normal 20 °C isotherm in the western Pacific is consistent with a developing La Niña event.

Figure 7 shows a cross-section of monthly equatorial sub-surface anomalies from May to August 2010 (obtained from CAWCR). Red shading indicates positive anomalies, and blue shades indicate negative anomalies. The sub-surface cross-section shows cool anomalies across the central and eastern Pacific in place in May, with autumn having seen

Fig. 7 Four-month (May to August 2010) sequence of vertical sea subsurface temperature anomalies at the equator for the Pacific Ocean. The contour interval is 0.5 °C.

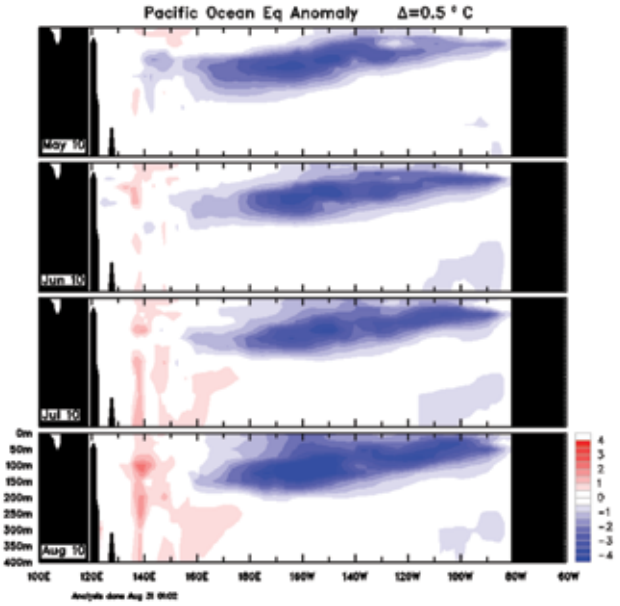

[7]Hovmöller plot obtained from http://www.pmel.noaa.gov/tao/jsdisplay/

a rapid transition from warm to cool anomalies in this region (Campbell 2011). During the winter months, the cool anomalies intensified, and spread towards the surface, so that by August most of the central and eastern Pacific had strong cool anomalies. The western Pacific warmed slightly during winter, to have weak warm anomalies by August.

Global atmospheric patterns

Surface analyses

The southern hemisphere winter 2010 MSLP pattern, computed from the Bureau of Meteorology's Australian Community Climate and Earth-System Simulator[8] (ACCESS) model (the previous GASP model having been phased out in August 2010), is shown in Fig. 8, with the associated anomaly pattern shown in Fig. 9. These anomalies are the difference from a 1979–2000 climatology obtained from the National Centers for Environmental Prediction (NCEP) II Reanalysis data (Kanamitsu et al. 2002). The MSLP analysis has been computed using data from the 0000 UTC daily analyses of the ACCESS model. The MSLP anomaly field is not shown over areas of elevated topography (grey shading).

Showing a weak three-wave structure, the winter MSLP pattern was zonal in the mid to high latitudes, with troughs located at approximately 90°E, 120°W and 15°W. Anomalous high pressure occurred over the southern Indian Ocean and the central southern Pacific Ocean, and the MSLP was slightly above average over the Australian region, with anomalies of +5.0 hPa just off the far southwest tip of Australia. Anomalous low pressure occurred over the Antarctic region. This pattern has strong similarities to the loading pattern of the Southern Annular Mode (SAM) which is discussed in more detail in a following section.

Mid-tropospheric analyses

The 500 hPa geopotential height, which is an indicator of the steering of surface synoptic systems across the southern hemisphere, is shown in Fig. 10 for June to August. The associated anomalies are shown in Fig. 11. Figure 10 shows that the winter 500 hPa height pattern displays the characteristic zonal structure in the mid to high latitudes, with weak three-wave characteristics, that were also noted in Fig. 8.

Southern Annular Mode

The Southern Annular Mode (SAM) describes the periodic, approximately ten-day, oscillation of atmospheric pressure between the polar and mid-latitude regions of the southern hemisphere. Positive phases of SAM are characterised by increased mass over the extra-tropics, decreased mass over Antarctica and a poleward contraction of the mid-latitude band of westerly winds. Conversely, negative phases of SAM relate to reduced mass over the extra-tropics, increased mass over Antarctica and an equatorward expansion of the mid-latitude band of westerly winds. A similar oscillation exists in the northern hemisphere, the Northern Annular Mode, or NAM. After being slightly positive during autumn, the Climate Prediction Center standardised monthly SAM index (Climate Prediction Center 2010) became very strongly positive in winter. In fact, June's value of +2.07 was the strongest positive June value on record (records began in 1979), as was July's +2.42. The August value of +1.51 was second strongest on record.

Figures 9 and 11 indicate anomalously high pressure for winter 2010 around the mid-latitudes in the southern Indian Ocean and Pacific Ocean regions and anomalously low pressure over the Antarctic region. As discussed in an earlier section, this pattern is strongly similar to the loading pattern for positive SAM. Hendon et al. (2007) discusses Australian rainfall patterns associated with the positive and negative phases of SAM. Their findings report that the positive phase of SAM is usually associated with decreased westerly flow

Fig. 8 Southern hemisphere winter 2010 MSLP (hPa). The contour interval is 5 hPa.

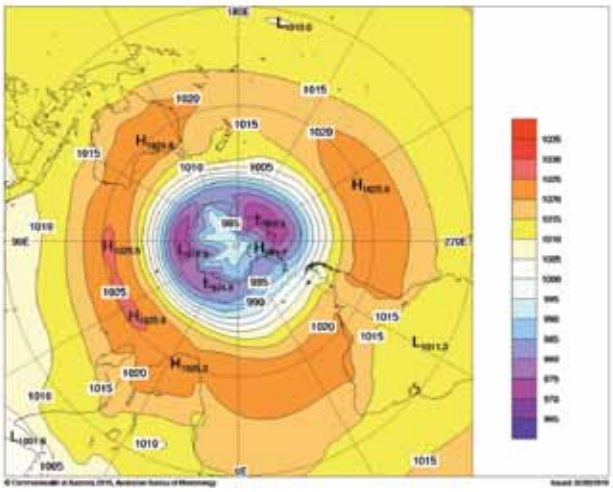

Fig. 9 Southern hemisphere winter 2010 MSLP anomalies (hPa). The contour interval is 2.5 hPa.

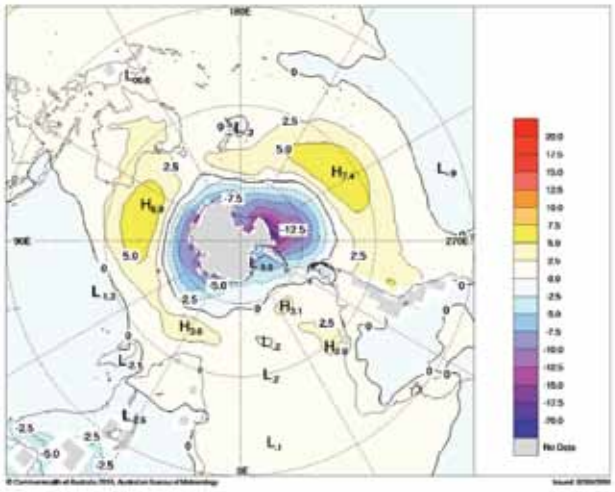

[8]For more information on the Bureau of Meteorology's ACCESS model, see http://www.bom.gov.au/nwp/doc/access/NWPData.shtml

in the southern regions of Australia. The positive SAM is likely to have played a strong part in the southwest Western Australian region having its lowest winter rainfall on record. In the southeast of Australia the developing La Niña offset drying from the SAM effect. Otherwise, no other climatic effects of the SAM were observed in Australia.

Blocking

The time-longitude section of the daily southern hemisphere blocking index (BI, Wright 1993) is shown in Fig. 12, with the start of the season beginning at the top of the plot. This index is a measure of the strength of the zonal 500 hPa flow in the mid-latitudes (40ºS to 50ºS) relative to that at lower (25ºS to 30ºS) and higher (55ºS to 60ºS) latitudes. Positive values of the blocking index are generally associated with a split in the mid-latitude westerly flow centred near 45ºS and mid-latitude blocking activity. Blocking activity most commonly occurs in the Australian and western Pacific latitudes. Fig. 13 shows the seasonal index for each longitude.

The seasonal index shows that blocking was above average in most areas, apart from the eastern Pacific region. Positive daily BI values were fairly consistent throughout the winter season between 120ºE to 150ºW, with the strongest values in the 150ºE to 180ºE longitudes (approximately the Tasman Sea region).

Winds

Winter 2010 low-level (850 hPa) and upper-level (200 hPa) wind anomalies (as per the surface analyses, computed from ACCESS and anomalies with respect to the 22-year NCEP II climatology) are shown in Fig. 14 and 15, respectively. Istotach contours are at 5 ms^{-1} intervals.

Fig. 10 Southern hemisphere winter 2010 500 hPa mean geopotential height (gpm). The contour interval is 100gpm.

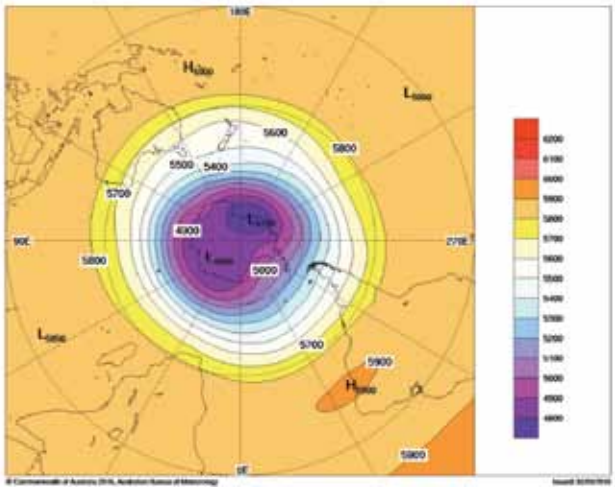

Fig. 11 Southern hemisphere winter 2010 500 hPa mean geopotential height anomaly (gpm). The contour interval is 30 gpm.

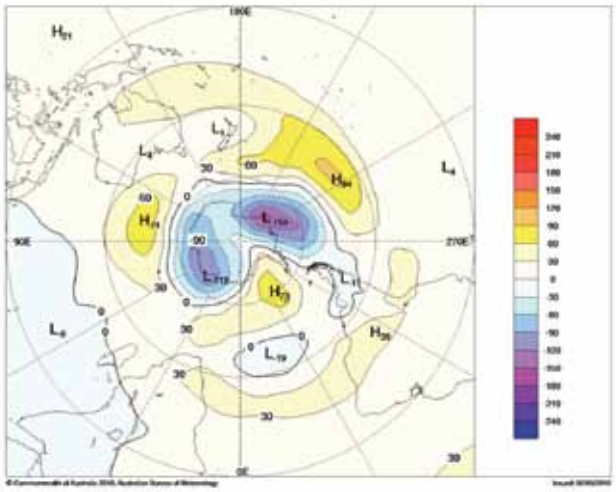

Fig. 12 Winter 2010 daily blocking index time-longitude section. Day 1 is 1 June.

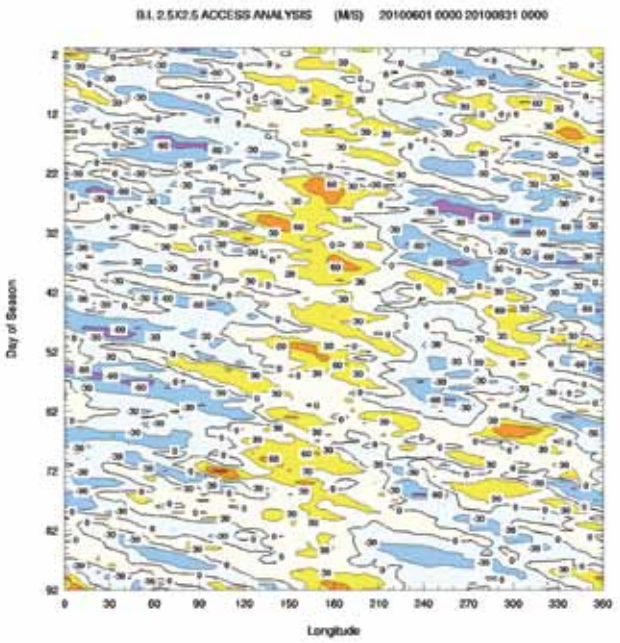

Fig. 13 Mean southern hemisphere blocking index for winter 2010 (solid line). The dashed line shows the corresponding long-term average. The horizontal axis shows the degrees east of the Greenwich meridian.

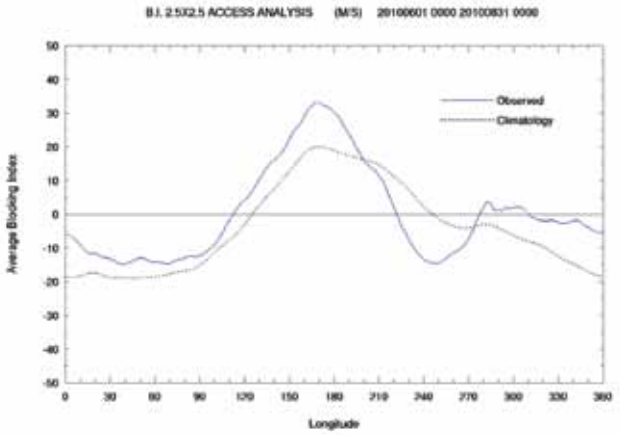

Fig. 14 Global winter 2010 850 hPa vector wind anomalies (ms^{-1}).

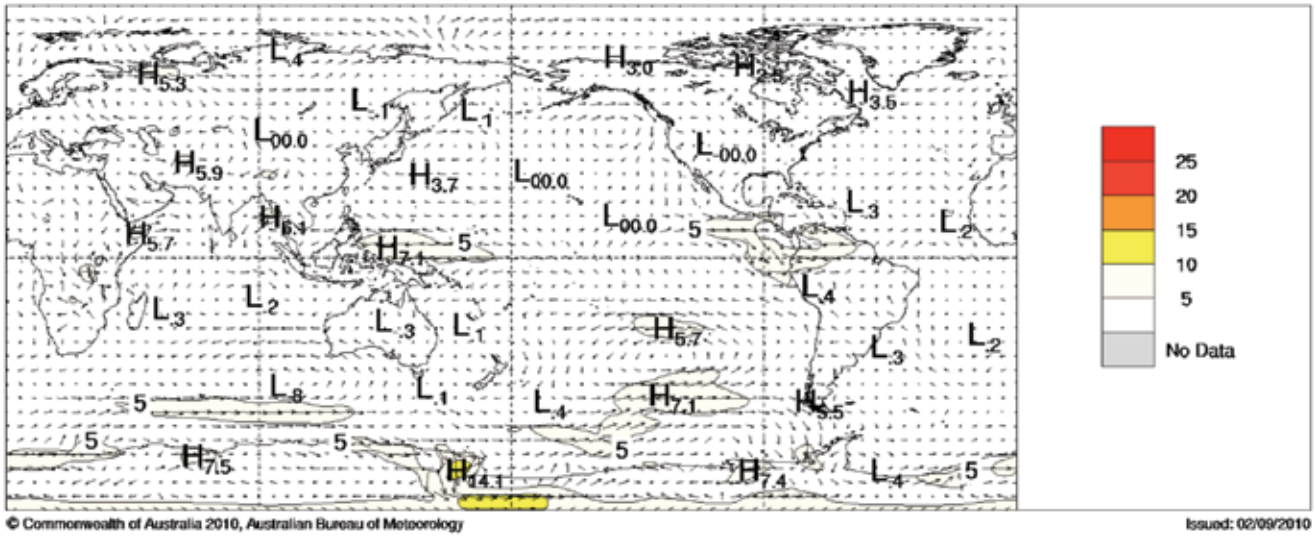

Fig. 15 Global winter 2010 200 hPa vector wind anomalies (ms^{-1}).

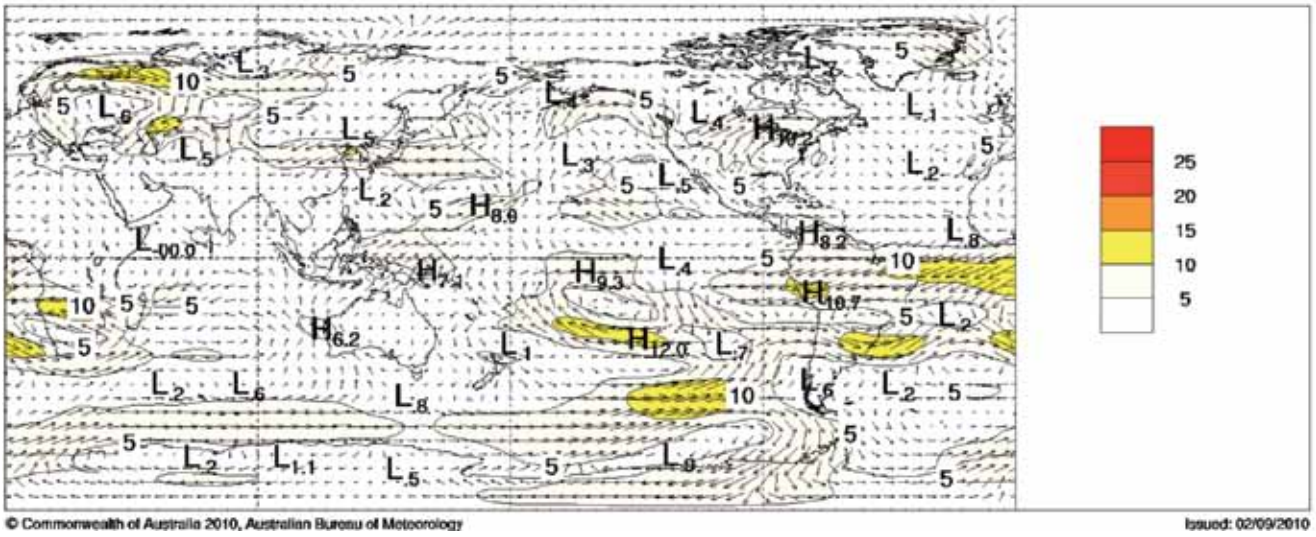

The low-level winds generally reflected the MSLP anomalies shown in Fig. 9, including an anticyclonic anomaly over the southern Indian Ocean, to the southwest of Western Australia. The enhanced easterlies over the western to central Pacific (anomalies reached 7 ms^{-1} near Papua New Guinea), in combination with enhanced upper-level westerlies across the same region, were indicative of a stronger than normal Walker Circulation (La Niña).

Upper-level westerly anomalies between 0ºE and 90ºW were consistent with a southward shift in the polar-front jet. This is in-turn consistent with the positive SAM.

Australian region

Rainfall

Australian rainfall totals for winter are shown in Fig. 16, while the rainfall deciles for the same period are shown in Fig. 17. The rainfall deciles are calculated using all winters from 1900 to 2010.

Overall, Australia had a wetter than normal winter, with an area-average of 77.6 mm, 21 per cent above the long-term average (1961–1990). Winter 2010 rainfall was the 26th highest out of 111 years. Figure 17 shows that most regions received average to above average falls. Higher than normal falls generally occurred in the north and east of the country. A large band of decile 10 rainfall extended from the Kimberley, into the southern half of the Northern Territory and northern South Australia, and through to the eastern Queensland and New South Wales border region. Small areas near Derby in Western Australia, Alice Springs in the Northern Territory and Moomba in South Australia had record high falls. An area of western Victoria between Ballarat and Warrnambool registered falls in the highest decile, as did small areas in the Top End of the Northern Territory and the far north

Peninsula region of Queensland, where a small area of the eastern tip was highest on record.

Southern Tasmania and the far southeast mainland of Australia had below average falls. Southwest Western Australia (a region southwest of a line joining Jurien Bay and Bremer Bay) had its driest winter on record by a substantial margin, with an area-average of 184.6 mm (previously 214.5 mm, set in 1914). The area surrounding this region was also very dry, with much of it in decile 1.

Nationally, June was particularly dry (fourth-driest on record for Australia), while July and August were much wetter in comparison.

Fig. 16 Winter 2010 rainfall totals (mm) for Australia.

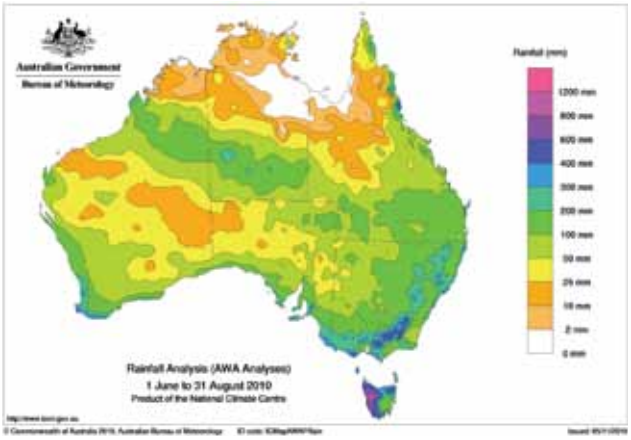

Drought

As discussed in the previous section, rainfall was below to very much below average across southwestern Australia, southern Tasmania and the far southeast of mainland Australia. Persistent dry weather in southwest Western Australia produced the driest winter on record for the southwest Western Australia region as a whole. Further east, rainfall has generally been average to above average since late 2009 for northern and eastern Australia, alleviating any previous short-term rainfall deficiencies.

A way in which the Bureau of Meteorology presently assesses drought is by considering the extent of areas of the country which contain accumulated rainfall in the lowest decile for varying timescales. To the end of August 2010, local

Fig. 17 Winter 2010 rainfall deciles for Australia: decile ranges based based on grid-point values over the winter periods from 1900 to 2010.

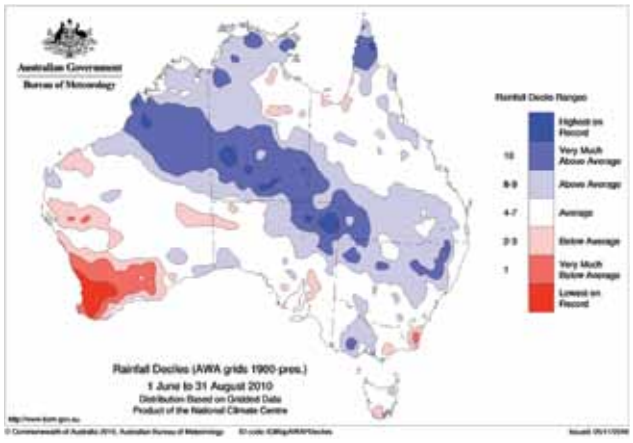

Table 1. Summary of the seasonal rainfall ranks and extremes on a national and State basis for winter 2010. The ranking in the last column begins from 1 (lowest) to 111 (highest) and is calculated over the years 1900 to 2010 inclusive.

Region	*Highest seasonal total (mm)*	*Lowest seasonal total (mm)*	*Highest daily total (mm)*	*Area-averaged rainfall (mm)*	*Rank of area-averaged rainfall*
Australia	1848.6 at Bellenden Ker Top St (Qld)	Zero at several locations	277.0 at Bellenden Ker Top St (Qld) on 31/08	77.6	86
Western Australia	477.8 at Forest Grove	Zero at Faraway Bay and Parry Creek Farm	135.0 at Ningaloo on 16/06	60.3	60
Northern Territory	186.4 at Yuendumu	Zero at several locations	119.0 at Idracowra on 13/07	52.8	107
South Australia	605.4 at Piccadilly	15.1 at Olary (Wiawera)	69.2 at Marree on 13/07	66.7	75
Queensland	1848.6 at Bellenden Ker Top St	Zero at several locations	277.0 at Bellenden Ker Top St on 31/08	68.3	83
New South Wales	774.1 at Thredbo Village	25.2 at Bemboka	247.0 at Meerschaumvale on 03/06	137.1	81
Victoria	905.0 at Weeaproinah	58.9 at Pirlta	110.0 at Weeaproinah on 12/08	217.7	74
Tasmania	1120.2 at Mt Read	71.6 at Seven Mile Beach	199.4 at Mt Wellington on 12/08	423.9	48

temporal maxima in the areal extent of rainfall deficiencies occurred at periods of 8, 17, 28, 40, 52 and 68 months. For the 8-month period ending August 2010, 8.4 per cent of Australia, including 25.2 per cent of Western Australia and 19.5 per cent of Tasmania, were experiencing serious rainfall deficiencies (i.e. rainfall totals below the tenth percentile). For the western half of Western Australia, these deficiencies were a result of general dryness over an extended period, while in southern Tasmania, the deficiencies were residual deficiencies from a very dry January-July. Very much above average rainfall during August eased deficiencies somewhat in southern Tasmania.

For the 17-month period ending August 2010, 9.6 per cent of Australia, or 29.3 per cent of Western Australia and 1.8 per cent of Tasmania were experiencing serious rainfall deficiencies. The 17-month rainfall deficiencies extended further east across the southwest region of Western Australia compared to the 8-month period, while the Gascoyne and Pilbara regions of Western Australia had a wider extent of severe deficiencies (i.e. rainfall totals below the 5th percentile) in the longer period.

The deficiencies discussed above occurred against a backdrop of decade-long rainfall deficits and high temperatures that have stressed water supplies, particularly in the southwest and southeast regions of Australia. For the 68-month period ending August 2010, 8.1 per cent of Australia experienced serious rainfall deficiencies. The States which made notable contributions to this area are Tasmania (74.7 per cent of its area), Victoria (64.9 per cent), New South Wales (10.0 per cent) and Western Australia (8.1 per cent).

Temperature

Figure 18 shows maximum and minimum temperature anomalies for winter. Seasonal anomalies are calculated with respect to the 1961–1990 period, and use all stations for which an elevation is available. Station normals have been estimated using gridded climatologies for those stations with insufficient data within the 1961–1990 period to calculate a station normal directly. Figure 19 shows maximum and minimum temperature deciles, calculated using monthly temperature analyses from 1911 to 2010.

Fig. 18 Winter 2010 temperature anomalies (°C) for Australia: anomalies based on a 1961-1990 mean. (a) Maximum temperature anomalies and (b) minimum temperature anomalies.

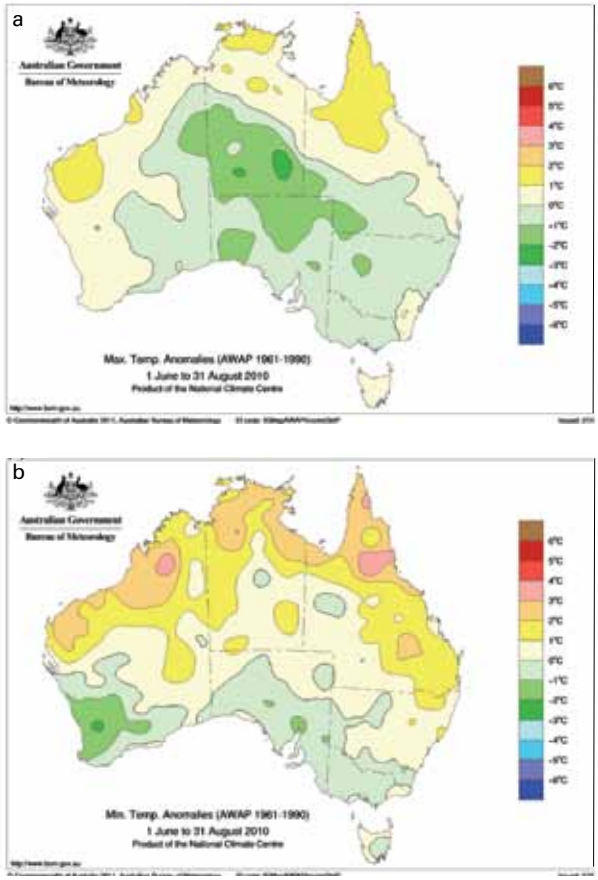

Fig. 19 Winter 2010 temperature deciles for Australia: decile ranges based on grid-point values over the winter periods for 1900 to 2010. (a) Maximum temperature deciles and (b) minimum temperature deciles.

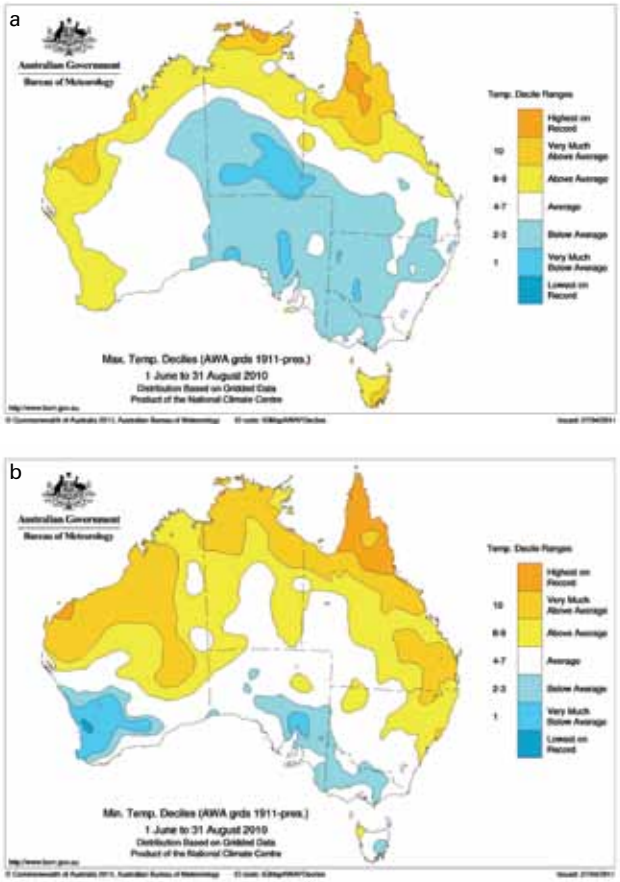

Winter mean maximum temperatures were above normal in the western half of Western Australia, the northern half of the Northern Territory, northern and eastern Queensland, the far southeast of New South Wales and over Tasmania. Anomalies in excess of +1 °C were recorded in the Pilbara region and a small area of the western Kimberley in Western Australia, as well as the north of the Northern Territory and northern Queensland. Parts of the Top End of the Northern Territory and the Cape York Peninsula recorded their highest winter maxima on record (Fig. 19). Tasmania as a whole was unseasonably mild, recording its seventh warmest winter maximum temperatures.

Below normal maxima covered most of the central and southern regions of Australia. Anomalies below 1 °C were recorded in an area of central Australia, covering the southern Northern Territory and northern South Australia, extending across the borders into Western Australia, Queensland and New South Wales. Small areas near Alice Springs were over 2 °C below normal. South Australia as a whole was rather cool, recording its ninth coolest winter maxima. Australia had a close to normal winter, with an area averaged anomaly of –0.01 °C. Nevertheless, nationally it was the coolest winter maximum since 1997 (13 years).

Minimum temperatures for winter were generally above average in the north of the country and below average in the south. Anomalies of +1 to +3 °C covered large areas of northern Australia, with the strongest anomalies generally close to the northern coastline. The far northern coast and offshore islands were especially warm; Cape Don (NT) set an Australian July record of 26.9 °C, while Horn Island and Coconut Island, in the Torres Strait, broke the previous Queensland August record on 24 occasions between them. An area of the Pilbara coast in Western Australia and most of the Cape York Peninsula in Queensland had their warmest mean winter minima on record. Queensland as a whole was also rather warm, recording an anomaly of +1.18 °C, its eighth warmest winter minima.

In southwest Western Australia and small areas near Port Augusta and Tarcoola in South Australia, minimum temperatures were 1 to 2 °C below average. These areas were in the lowest decile, with a small area near Perth recording its lowest winter minima on record. The southwest Western Australian region as a whole had their third coolest mean winter minima. Combined with the above average daytime temperatures, the resulting third-highest diurnal temperature range highlighted the drought conditions in this part of the country.

Table 2. Summary of the seasonal maximum temperature ranks and extremes on a national and State basis for winter 2010. The ranking in the last column begins from 1 (lowest) to 61 (highest) and is calculated over the years 1950 to 2010.

Region	*Highest seasonal mean maximum (ºC)*	*Lowest seasonal mean maximum (ºC)*	*Highest daily temperature (ºC)*	*Lowest daily maximum temperature (ºC)*	*Area-averaged temperature anomaly (ºC)*	*Rank of area-averaged temperature anomaly*
Australia	34.2 at Noonamah (NT)	0.0 at Mt Hotham (Vic)	39.0 at Wyndham (WA) on 20/08 and at Bradshaw (NT) on 25/08	–5.3 at Mt Hotham (Vic) on 28/06	–0.01	24
Western Australia	32.6 at Wyndham	15.0 at Rocky Gully	39.0 at Wyndham on 20/08	9.0 at Mt Barker on 18/08	+0.25	34
Northern Territory	34.2 at Noonamah	18.2 at Kulgera	39.0 at Bradshaw on 25/08	6.7 at Arltunga on 06/07	–0.46	17
South Australia	19.3 at Marree Comparison	9.5 at Mt Lofty	28.4 at Ceduna on 31/08	5.7 at Mt Lofty on 04/08	–0.87	9
Queensland	32.9 at Kowanyama	14.6 at Applethorpe	37.2 at Julia Creek on 19/08	8.1 at Charleville on 07/07	+0.54	38
New South Wales	21.3 at Grafton Olympic Pool	0.4 at Thredbo Top Station	29.9 at Bourke on 18/08	–4.6 at Thredbo Top Station on 25/08	–0.18	18
Victoria	15.4 at Mildura	0.0 at Mt Hotham	21.5 at Mildura on 31/08	–5.3 at Mt Hotham on 28/06	–0.18	21
Tasmania	15.1 at Bicheno	3.2 at Mt Wellington	18.4 at Bicheno on 12/07 and at Hobart on 15/08	–2.0 at Mt Wellington on 16/08	+0.97	55

Table 3. Summary of the seasonal minimum temperature ranks and extremes on a national and State basis for winter 2010. The ranking in the last column begins from 1 (lowest) to 61 (highest) and is calculated over the years 1950 to 2010.

Region	*Highest seasonal mean minimum (ºC)*	*Lowest seasonal mean minimum (ºC)*	*Highest daily minimum temperature (ºC)*	*Lowest daily temperature (ºC)*	*Area-averaged temperature anomaly (ºC)*	*Rank of area-averaged temperature anomaly*
Australia	25.4 at Coconut Island (Qld)	–6.1 at Charlotte Pass (NSW)	26.9 at Cape Don (NT) on 26/07	–19.6 at Charlotte Pass (NSW) on 20/07	+0.56	50
Western Australia	24.1 at Troughton Island	2.0 at York	26.4 at Troughton Island on 02/06	–6.8 at Eyre on 11/08	+0.55	49
Northern Territory	24.5 at Cape Don	5.2 at Arltunga	26.9 at Cape Don on 26/07	–2.7 at Alice Springs on 15/06 and at Arltunga on 15/06	+0.39	40
South Australia	10.1 at Cape Willoughby	2.1 at Yongala	16.8 at Moomba on 30/07	–4.5 at Renmark on 06/07	+0.17	34
Queensland	25.4 at Coconut Island	3.5 at Stanthorpe	26.8 at Horn Island on 19/08	–6.0 at Oakey on 28/06	+1.18	54
New South Wales	11.4 at Smoky Cape	–6.1 at Charlotte Pass	19.2 at Cape Byron on 31/07	–19.6 at Charlotte Pass on 20/07	+0.27	37
Victoria	9.4 at Wilsons Promontory	–3.9 at Mt Hotham	13.5 at Moorabbin on 25/06	–8.2 at Mount Hotham Airport on 20/07	–0.26	15
Tasmania	8.4 at Swan Island	–1.4 at Liawenee	13.3 at Eddystone Point on 25/06	–7.9 at Liawenee on 25/07	+0.28	40

References

Campbell, B. 2011. Seasonal climate summary southern hemisphere (autumn 2010): rapid decay of El Niño, wetter than average in central, northern and eastern Australia and warmer than usual in the west and south. *Aust. Met. Oceanogr. J., 61,* 65-76.

Climate Diagnostics Center. 2010. *Historical ranks of the MEI,* http://www.cdc.noaa.gov/people/klaus.wolter/MEI/rank.html.

Climate Prediction Center. 2010. *Monthly mean AAO index since January 1979,* http://www.cpc.noaa.gov/products/precip/CWlink/daily_ao_index/aao/aao.shtml.

Donald, A., Meinke, H., Power, B., Wheeler, M. and Ribbe, J. 2004. Forecasting with the Madden-Julian Oscillation and the applications for risk management. In *4th International Crop Science Congress,* 26 September – 01 October 2004, Brisbane, Australia.

Hendon, H.H., Thompson, D.W.J. and Wheeler, M.C. 2007. Australian Rainfall and Surface Temperature Variations Associated with the Southern Hemisphere Annular Mode. *J. Clim., 20,* 2452-67.

Kanamitsu, M., Ebisuzaki, W., Woollen, J., Yang, S.-K., Hnilo, J.J., Fiorino, M. and Potter, G.L. 2002. NCEP-DOE AMIP-II Reanalysis (R-2). *Bull. Am. Meteorol. Soc., 83,* 1631-43.

Kuleshov, Y., Qi, L., Fawcett, R. and Jones, D. 2008. On tropical cyclone activity in the Southern Hemisphere: trends and the ENSO connection. *Geophys. Res. Lett., 35,* L14S08, doi:10.1029/2007GL032983

Reynolds, R.W., Rayner, N.A., Smith, T.M., Stokes, D.C. and Wang, W. 2002. An improved in situ and satellite SST analysis for climate. *J. Clim., 15,* 1609-25.

Tobin, S. 2010. Seasonal climate summary southern hemisphere (summer 2009-2010): an El Niño summer; wetter than average for east, north and central areas, dry in Western Australia and Tasmania. *Aust. Met. and Oceanogr. J., 60,* 289-99.

Troup, A.J. 1965. The Southern Oscillation. *Q. J. R. Meteorol. Soc., 91,* 490-506.

Wolter, K. and Timlin, M.S. 1993. Monitoring ENSO in COADS with a seasonally adjusted principal component index. *Proc. of the 17th Climate Diagnostics Workshop,* Norman OK, NOAA/NMC/CAC, NSSL, Oklahoma Clim. Survey, CIMMS and the School of Meteorology, Univ. of Oklahoma, 52-7.

Wolter, K. and Timlin, M.S. 1998. Measuring the strength of ENSO – how does 1997/98 rank? *Weather, 53,* 315-24.

Wright, W.J. 1993. Seasonal climate summary southern hemisphere (autumn 1992): signs of a weakening ENSO event. *Aust. Meteorol. Mag., 42,* 191-8.